

# A Self-Tuning PI Control System Design for the Flatness of Hot Strip in Finishing Mill Processes

**Jeong Ju Choi**

*Department of Mechanical and Intelligent Systems Engineering, Pusan National University,  
Busan 609-735, Korea*

**Wan Kee Hong**

*Research Institute of Industrial Science & Technology, Pohang 790-330, Korea*

**Jong Shik Kim\***

*School of Mechanical Engineering and RIMT, Pusan National University,  
Busan 609-735, Korea*

A novel flatness sensing system which is called the Flatness Sensing Inter-stand Looper (FlatSIL) system is suggested and a self-tuning PI control system using the FlatSIL is designed for improving the flatness of hot strip in finishing mill processes. The FlatSIL system measures the tension along the direction of the strip width by using segmented rolls, and the tension profile is approximated through the tension of each segmented roll. The flatness control system is operated by using the tension profile. The proposed flatness control system as far as the tension profile-measuring device works for the full strip length during the strip rolling in finishing mills. The generalized minimum variance self-tuning (GMV S-T) PI control method is applied to control the flatness of hot strip which has a design parameter as weighting factor for updating the PI gains. Optimizing the design parameter in the GMV S-T PI controller, the Robbins-Monro algorithm is used. It is shown by the computer simulation and experiment that the proposed GMV S-T PI flatness control system has better performance than the fixed PI flatness control system.

**Key Words :** Flatness, Hot Rolling Process, Generalized Minimum Variance Self-Tuning PI Control

## 1. Introduction

Rolling process is a continuous process for making thin strips through reducing the thickness of strips that pass the rolling stand interval consisted of several rolls. At the present time, the specifications of hot strip such as thickness, width and flatness of strip are more precisely required. One of them, the specification of flatness is more

important in the hot strip market (Yi et al., 2001) because the flatness in hot rolling processes affects the thinner hot strip productivity as well as it is important to the workability improvement of cold rolling as the previous process of cold rolling.

The flatness of strip in finishing mills depends on the tension distribution. When a strip is rolled, the tension distribution is affected by the flatness degree and the bad flatness of strip frequently happens in thinner strip products. Therefore, the proper flatness control system should be settled in finishing mill processes. However, the systematic control system based on the mathematical model has not been developed, because it is very difficult to physically describe the dynamic behavior between the bender pressure that performed as the

---

\* Corresponding Author,  
E-mail : jskim@pusan.ac.kr  
TEL : +82-51-510-2317; FAX : +82-51-510-3077  
School of Mechanical Engineering and RIMT, Pusan National University, Busan 609-735, Korea. (Manuscript Received April 18, 2003; Revised January 8, 2004)

input and the flatness of strip which is the output of the system.

For measuring the strip flatness, the direct and indirect measurement methods are used (Xilin et al., 1997). The indirect method usually uses a laser sensor and camera systems. The laser beam can only recognize the quality of the flatness, because the distance from the sensor to a hot strip is converted to the flatness. The direct method can measure the tension of strip precisely with separated rolls. The coarse surrounding effects easily damage the detailed separate rolls, and the life cycle of the sensor becomes short. Moreover, the bender, which is a hydraulic actuator, cannot precisely control the tension of hot strip.

Thus, an improved looper system, which is called the FlatSIL system, has been developed. The developed FlatSIL system can complement the previous sensing measurement and it extends the life cycle of measurement devices. The FlatSIL system estimates the tension profile in the lateral direction and approximates the tension profile as a quadratic equation and monitors the flatness of hot strip by using a coefficient of the quadratic equation. For the flatness control using the FlatSIL system, the coefficient of quadratic equation for the flatness of hot strip is used.

In this paper, to improve the performance of the flatness control based on the FlatSIL system, the GMV S-T PI controller is designed (Yamamoto, 1999), and the Robbins-Morno algorithm is used to optimize a weighting factor of the GMV S-T PI control. The dynamic behaviors of the flatness of hot strip is presented as a SISO system whose input is the bender and output is the flatness of strip. In order to show the excellence of the GMV S-T PI control system, computer simulation and experimental results are shown.

## 2. Measurement of the Flatness of Hot Strip

The FlatSIL system measures the tension of strip and converts to the profile of tension in the lateral direction. It consists of five separated segment rolls that are three measuring segment rolls and two dummy ones. The concept of seg-

mentation is to detect the tension profile across the strip width. The new design of reduced number of segments is to assure the longer life of the device under the severe environment of inter-stand space and easy maintenance. The three-segmented measuring rolls are only adopted to get a wave pattern of hot strip between stands. Each segmented roll has a load cell at the position of both barrel ends, and the two load values acting on the individual segmented roll are used for calculating the average load value over the span of strip in contact with the segmented roll. The position of the strip over the looper roll is measured by a width-meter installing behind the last stand. With three rolls, we can determine whether the pattern of the tension profile is concave or convex. Based on the measured tension values, we can formulate a basic correlation between the tension profile pattern and the strip wave. The limitation of the three-point curve fitting is justified here, because the hot strip mill has only a symmetric control actuator of the work roll bender and the curve form of the tension profile is enough to determine the bending direction.

Fig. 1 shows the configuration of the FlatSIL system. In order to setup the FlatSIL system, the traditional full-length looper roll is replaced by separated segment rolls with its own bearings. Each axis of the segmented roll has its own bearings and each bearing assembly is pivoted, to transfer the strip tension on the segmented roll to the load cell. The segmented rolls can easily be separated from the looper table by just unbolting the bearing shield covers of the roll shaft support. The load cells are encapsulated by the housing

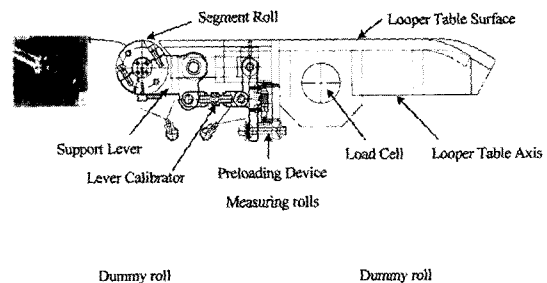


Fig. 1 Configuration of the FlatSIL system

block and cushioned by a shock-absorbing pad for protection from impact shock during the resetting of position of the looper table between coils. Coolant water is supplied to the segmented roll and the load cell housing. An important matter in the looper operation is the mass moment of inertia. The mechanical frame of the FlatSIL system was designed by considering the base torque and the wear resistance of the segmented roll since the segmented roll continuously contacts the running strip during the rolling processes. The present segmented roll is thermal-spray coated to increase wear resistance. The load acting on the segmented looper roll consists of the weight of strip, the bending force, the centrifugal force and the inertia force as well as the strip tension.

Figure 2 illustrates the load acting on the segmented roll separated by the radial force  $F_A$  and the tangential force  $F_L$ , where  $\theta_f$  is the looper angle and  $\theta_0$  is the angle between the strip pass line and the load-sensing direction of the segmented roll. For simplicity, we consider the static components of these forces under the assumption that the looper position is in a steady state. In order to calculate the strip tension from the measured load, the inertia effect is neglected and the geometric relation shown in Fig. 2 is used.

$$T = \frac{K_n \times F_{LC} - (K_j \sin \theta_f + K_k \sin \theta_f) \times (F_1 - F_2)}{W_{seg} \times h} \quad (1)$$

where

- $T$  : unit tension (kgf/mm<sup>2</sup>)
- $K_n$  : variable related to the looper angle (degree)

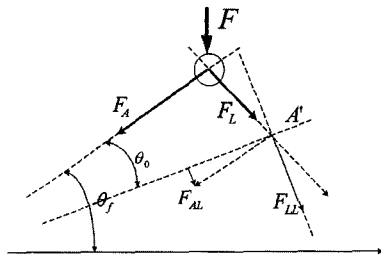


Fig. 2 Load acting on the segmented roll separated by the radial and tangential forces

- $F_{LC}$  : weight of the strip on the load cell (kgf)
- $K_j, K_k$  : constants related to the looper angle (degree)
- $\theta_f$  : looper angle (degree)
- $F_1$  : load of the strip bending and weight (kgf)
- $F_2$  : centrifugal force of strip (kgf)
- $W_{seg}$  : strip width on the segmented roll (mm)
- $h$  : exit thickness (mm)

To express the tension profile which is shown in Fig. 3 with the dotted line, the normalized values by the set-up tension  $T_n$  is expressed as the normalized values  $B_n, C_n$  and  $X_n$  as follows :

$$T_n = A_n + B_n X_n + C_n X_n^2 \quad (2)$$

where

$$B_n = \frac{1}{X_{Rn} - X_{Ln}} \left( \frac{X_{Rn}}{X_{Ln}} (T_{n1} - T_{n2}) - \frac{X_{Ln}}{X_{Rn}} (T_{n3} - T_{n2}) \right)$$

$$C_n = \frac{1}{X_{Rn} - X_{Ln}} \left( -\frac{1}{X_{Ln}} (T_{n1} - T_{n2}) + \frac{1}{X_{Rn}} (T_{n3} - T_{n2}) \right)$$

$$T_{n1} = A_n + B_n X_{Ln} + C_n X_{Ln}^2$$

$$T_{n2} = A_n, \quad T_{n3} = A_n + B_n X_{Rn} + C_n X_{Rn}^2$$

$$X_{Ln} = -\frac{W_{seg2} + W_{seg1}}{2} \times \frac{1}{X_{Lmax}}$$

$$X_{Rn} = -\frac{W_{seg2} + W_{seg3}}{2} \times \frac{1}{X_{Rmax}}$$

$B_n$  describes the linear component for skewing that means the level difference between strip sides which represents the side wave character, and  $C_n$  describes the difference of the normalized tensions between the strip center and sides which represents the flatness character.  $X_n$  is the normalized length of displacement of strip and  $W_{seg1}$ ,

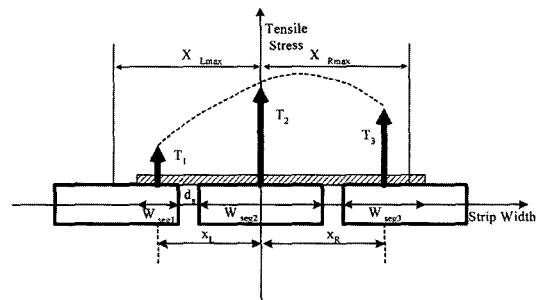


Fig. 3 Tension profile extracted from the load based on segmented roll

$W_{seg2}$  and  $W_{seg3}$  are the lengths of hot strip on the segmented rolls.

It is important that the flatness coefficients in the present work cannot represent the exact flatness of the strip edge, but the coefficients can indicate sufficiently the strip wave. We can predict the tension profile pattern by these coefficients and determine the control methods for the side wave and the flatness of strip with coefficients  $B_n$  and  $C_n$  respectively. For improving the flatness of hot strip, the coefficient  $C_n$  of the quadratic equation should be maintained as zero. Thus,  $C_n$  is selected as the output for the bender input, and the input-output relation is identified by the recursive least square (RLS) method.

### 3. Design of the GMV S-T Controller Using the Robins-Monro Algorithm

The FlatSIL system dynamics is assumed as a second order discrete regression model as follows :

$$y(t) = \phi^T(t) \theta \tag{3}$$

where

$$\theta = [a_0, a_1, a_2, b_0, b_1]^T$$

$$\phi = [y(t), y(t-1), y(t-2), u(t-1), u(t-2)]^T$$

And, the parameters  $\theta$  in Eq. (3) are estimated by the RLS with forgetting factor method.

$$\hat{\theta}(t) = \hat{\theta}(t-1) + L(t) [y(t) - \phi^T(t) \hat{\theta}(t-1)] \tag{4}$$

where

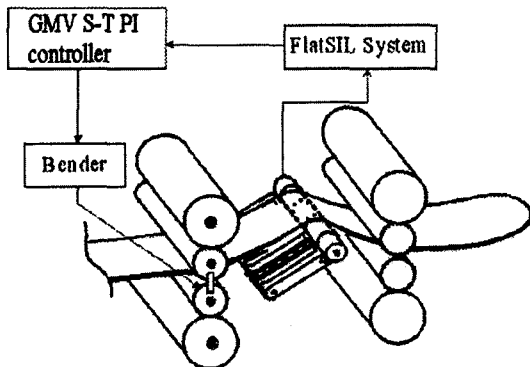


Fig. 4 Schematic of the GMV S-T PI flatness control system with the FlatSIL system

$$L(t) = \frac{P(t-1) \phi(t)}{\lambda_m + \phi^T(t) P(t-1) \phi(t)}$$

$$P(t) = \left[ P(t-1) - \frac{P(t-1) \phi(t) \phi^T(t) P(t-1)}{\lambda_m + \phi^T(t) P(t-1) \phi(t)} \right] / \lambda_m$$

$\lambda_m$  ( $0 < \lambda_m \leq 1$ ) is the forgetting factor.

In order to design the GMV S-T PI control system, the flatness control system is assumed by Eq. (5) and the schematic of the control system is shown in Fig. 4.

$$A(z^{-1}) y(t) = z^{-1} B(z^{-1}) u(t-1) + C(z^{-1}) \xi(t) \tag{5}$$

where  $A(z^{-1})$ ,  $B(z^{-1})$  and  $C(z^{-1})$  polynomials are represented by a shift operator  $z^{-1}$ , and  $\xi(t)$  is the uncorrelated random noise. And the auxiliary function for the GMV controller is defined as follows :

$$\phi(t) = P(z^{-1}) y(t) + Q(z^{-1}) u(t-1) - R(z^{-1}) y_r(t-1) \tag{6}$$

where  $y_r$  is the reference signal and  $P(z^{-1})$ ,  $Q(z^{-1})$  and  $R(z^{-1})$  are weighting polynomials.

If the input-output data are known until time 't', the auxiliary  $\phi(t+1)$  can be regarded as estimating  $\phi_y(t+1)$  as follows :

$$\phi_y(t+1) = P(z^{-1}) y(t+1) = \frac{F(z^{-1})}{C(z^{-1}) P_d(z^{-1})} y(t) + \frac{E(z^{-1}) B(z^{-1})}{C(z^{-1})} u(t) + E \xi(t+1) \tag{7}$$

where  $E(z^{-1})$  and  $F(z^{-1})$  are obtained by the Diophantine equation as follows (Gawthrop, 1986):

$$\frac{C(z^{-1}) P_n(z^{-1})}{A(z^{-1}) P_d(z^{-1})} = E(z^{-1}) + z^{-1} \frac{F(z^{-1})}{A(z^{-1}) P_d(z^{-1})} \tag{8}$$

where  $P_n(z^{-1}) / P_d(z^{-1}) = P(z^{-1})$ .

Recall Eq. (7) with  $G(z^{-1}) = E(z^{-1}) B(z^{-1})$  and  $C(z^{-1}) = 1$  is rewritten as follows :

$$\phi(t) = F(z^{-1}) y_f(t) + G(z^{-1}) u(t) + \varepsilon(t) \tag{9}$$

where  $\varepsilon(t) = E(z^{-1}) \xi(t+1)$  and  $y_f(t)$  is the filtered output and presented as follows :

$$y_f(t) = \frac{1}{P_d(z^{-1})} y(t)$$

where  $P_d(z^{-1})$  which can be arbitrarily chosen is represented as follows :

$$P_d(z^{-1}) = \frac{1+z^{-1}P_{d1}}{1+P_{d1}}, \quad (-1 < P_{d1} \leq 0)$$

The polynomials  $F(z^{-1})$  and  $G(z^{-1})$  can be estimated by the RLS method as  $\hat{F}(z^{-1})$  and  $\hat{G}(z^{-1})$  respectively. Therefore, the induced GMV control law is as follows :

$$u(t) = \frac{R(z^{-1})y_r(t) - \hat{F}(z^{-1})y_f(z^{-1})}{\hat{G}(z^{-1}) + Q(z^{-1})} \quad (10)$$

To design a GMV PI control law, a discrete PI control is constructed as follows :

$$\Delta u_{PI}(t) = K_p[e(t) - e(t-1)] + K_i e(t) \quad (11)$$

where  $\Delta$  is  $(1 - z^{-1})$ ,  $e(t) = y_r(t) - y(t)$  and  $K_p$  and  $K_i$  are the proportional and integral gains respectively. Eq. (11) can be rewritten by the filtered output  $y_f(t)$  as follows :

$$\Delta u(t) = K_i y_r(t) - (K_p + K_i) y_f(t) + K_p y_f(t-1) \quad (12)$$

The polynomial  $\hat{F}(z^{-1})$  in Eq. (10) is chosen as the first order polynomial to match Eq. (12).

$$\hat{F}(z^{-1}) = \hat{f}_0 + \hat{f}_1 z^{-1} \quad (13)$$

The polynomial  $R(z^{-1})$  is chosen for matching the reference output and the filtered output.

$$R(z^{-1}) = \hat{H} = \frac{F(z^{-1})}{P_d(z^{-1})} \Big|_{z=1} = \sum_{i=0}^1 \hat{f}_i \quad (14)$$

where  $\hat{f}_i$  are the coefficient of  $\hat{F}(z^{-1})$ , and the other polynomial  $Q(z^{-1})$  is represented as follows :

$$Q(z^{-1}) = \frac{1 - z^{-1}}{v} - \hat{G}(z^{-1}) \quad (15)$$

where  $v$  is a design parameter.

Eqs. (14) and (15) are substituted into Eq. (10). Then, the GMV S-T PI control law and the updating PI gains  $K_p$  and  $K_i$  are selected as follows :

$$\Delta u(t) = v[\hat{H}y_r(t) - \hat{y}_f(t)] \quad (16)$$

$$K_p = -v\hat{f}_1 \quad (17)$$

$$K_i = v(\hat{f}_0 + \hat{f}_1) \quad (18)$$

In this paper, to select a design parameter  $v$ , the Robbins-Monro algorithm which is the one of

stochastic approximation is used to optimize it. To obtain a update rule of the design parameter  $v$ , an expectation function  $E$  is constructed as a cost function and the cost function is optimized by the steepest descent method.

$$J = E[(Py_r(t) - \phi_y(t))^2] \quad (19)$$

And, the induced Robbins-Monro algorithm is as follows :

$$v(t) = v(t-1) + \mu(t) \left[ -\frac{\partial J}{\partial v} \right] \quad (20)$$

where  $\mu(t) = \frac{\mu_0}{t}$ , ( $0 < \mu_0 < 1$ ), and  $\frac{\partial J}{\partial v}$  can be presented by the chain rule as follows :

$$\frac{\partial J}{\partial v} = \frac{\partial J}{\partial \phi_y} \frac{\partial \phi_y}{\partial u} \frac{\partial u}{\partial v} \quad (21)$$

where

$$\begin{aligned} \frac{\partial J}{\partial \phi_y} &= -(Py_r(t) - \phi_y(t)), \quad \frac{\partial \phi_y}{\partial u} = \hat{g}_0 \\ \frac{\partial u(t)}{\partial v} &= \sum_{k=1}^t [\hat{H}_k y_r(t) - \hat{F}_k y_f(t)] \end{aligned}$$

and  $\hat{g}_0$  is a coefficient of  $\hat{G}(z^{-1})$ .

### 4. Simulation and Experiment

To evaluate the FlatSIL system, the value of coefficient  $C_n$  is divided into 20 zones, which are divided into 3 parts again. They are called the edge wave, the dead flat and the center wave. The flatness control maintains the coefficient  $C_n$  in the dead flat. Figure 5 shows the effect of the flat-

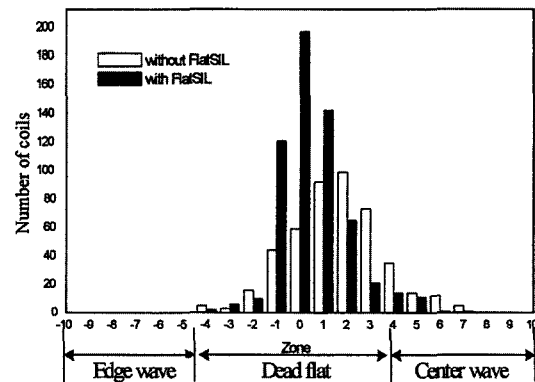


Fig. 5 Effect of the flatness control with/without the FlatSIL system

ness control with/without the FlatSIL system. For computer simulations, system dynamics were estimated that were performed based on the field data from POSCO at Kwangyang in Korea. The relations between the input and the output are shown in Fig. 6 through Fig. 8 which are sorted by the thickness of hot strip. The thickness of hot strip that is used in simulation is restrained less than 3.2t, because the bad flatness is apt to happen within this range.

The design parameter  $\nu$  for the GMV S-T PI

controller was chosen by the mathematical optimization techniques by the Robbins-Monro algorithm and by the trial and error method, and the coefficient  $P_{d1}(z^{-1})$  is selected as  $-0.46$ . Fig. 9 shows the GMV S-T PI control systems with/without the Robbins-Morno algorithm. As shown in Fig. 9, the GMV S-T PI control systems with the Robbins-Morno algorithm is faster than without it.

In order to apply the FlatSIL system to a continuous hot rolling process, two FlatSIL systems were installed between #5 and #6 and between #6

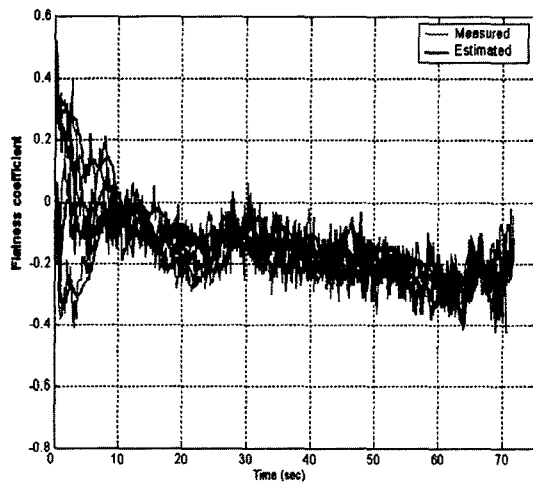


Fig. 6 Estimated flatness coefficients for the strip of 1.4t

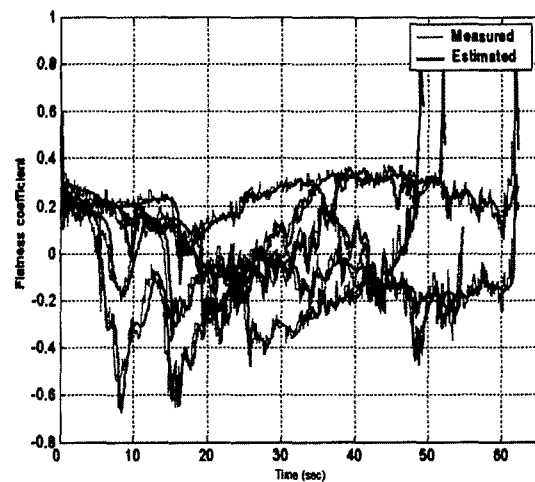


Fig. 8 Estimated flatness coefficients for the strip of 3.2t

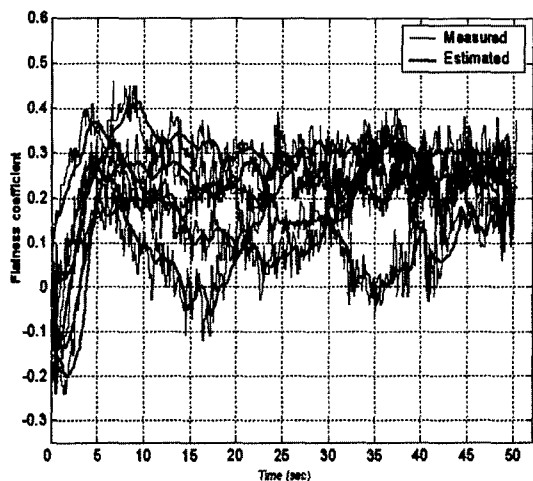


Fig. 7 Estimated flatness coefficients for the strip of 2.3t

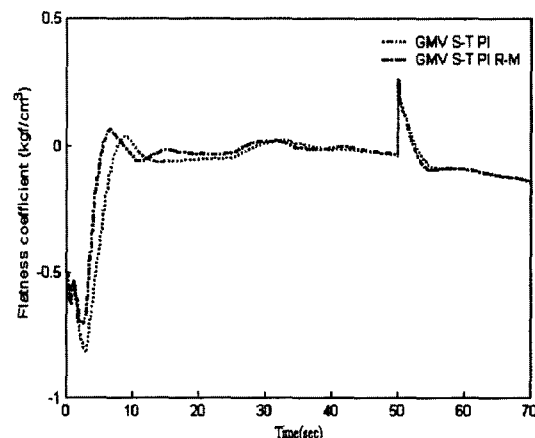


Fig. 9 GMV S-T PI control systems with/without the Robbins-Morno algorithm

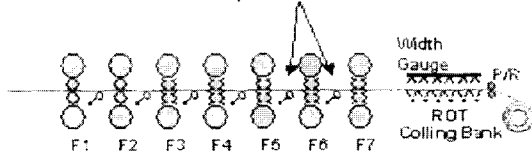
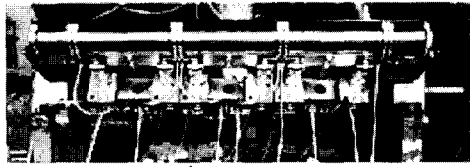


Fig. 10 Installation of the FlatSIL system

and #7 work rolls. Figure 10 shows the layout of the FlatSIL system. The designed GMV S-T PI controller was implemented to a real system and results are shown in Fig. 11 through Fig. 14. Figure 11 and 12 are for the fixed PI control system, and Figs. 13 and 14 are for the GMV S-T PI control system. The GMV S-T PI control system showed a better performance than the fixed PI control system. The results, however, at the #6 stand are worse than at the #5 stand in

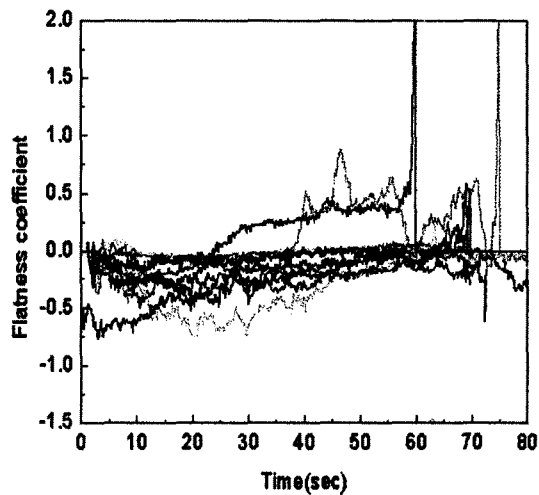


Fig. 11 Flatness coefficients in the #5 stand for the fixed PI control system

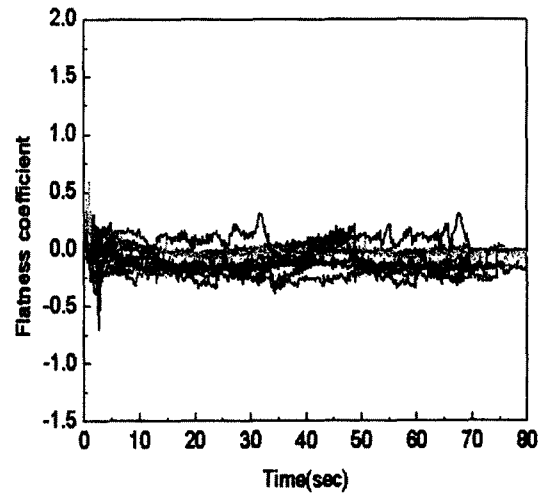


Fig. 13 Flatness coefficients in the #5 stand for the S-T PI control system

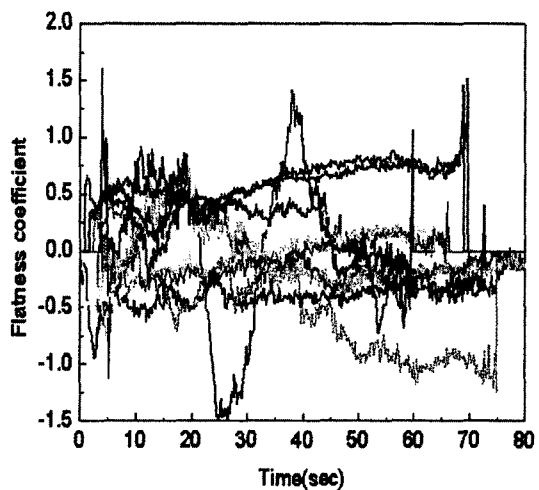


Fig. 12 Flatness coefficients in the #6 stand for the fixed PI control system

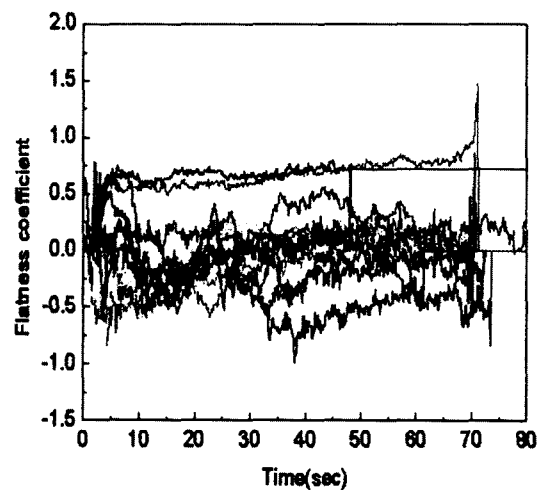


Fig. 14 Flatness coefficients in the #6 stand for the S-T PI control system

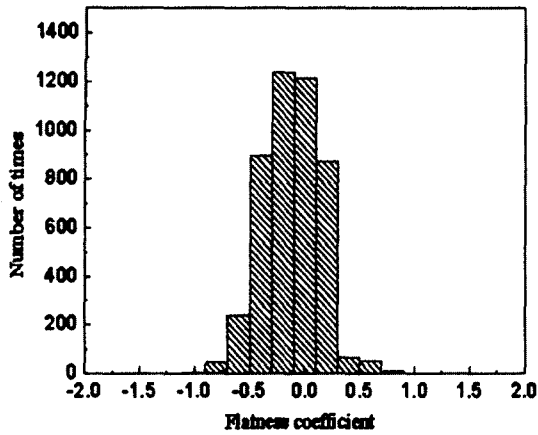


Fig. 15 Distribution of flatness coefficients for the fixed PI control system

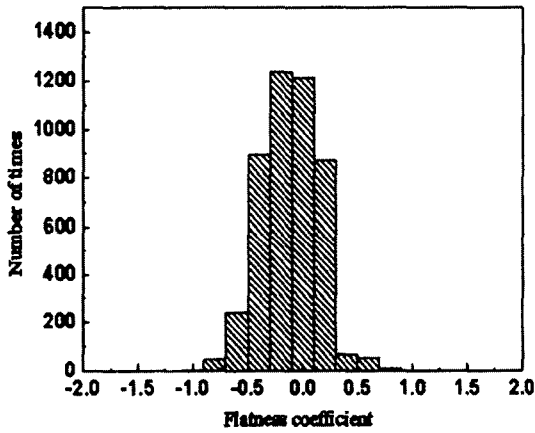


Fig. 16 Distribution of flatness coefficients for the S-T PI control system

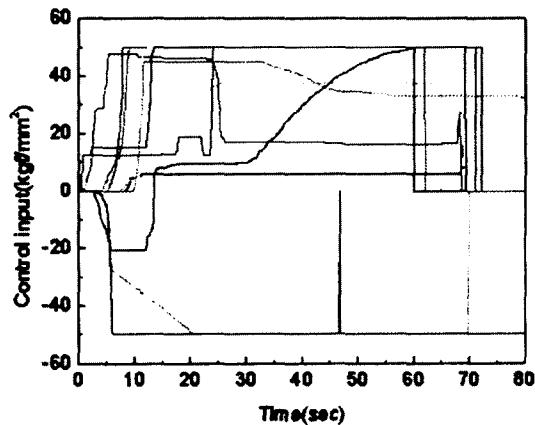


Fig. 17 Control inputs of the S-T PI control system in the #6 stand

the fixed and GMV S-T PI control systems simultaneously, because the hot strip becomes thinner after finishing the mill in the #5 stand.

Figs. 15 and 16 show the distribution of flatness coefficients for the fixed PI and GMV S-T PI control systems during the hot rolling processes, respectively. In the case of the GMV S-T PI control system, the range of distribution becomes narrower than the fixed PI control system. The standard deviations of the fixed and S-T PI control systems were 0.4056 and 0.2537, respectively. And, Fig. 17 shows the control inputs of the GMV S-T PI control system in the #6 stand. The control inputs were saturated frequently, because the capacity of the bender is insufficient. To improve the performance of the S-T controller, the capacity of the bender should be increased.

### 5. Conclusion

In this paper, the FlatSIL system is suggested for measuring the flatness of hot strip and the GMV S-T PI controller is designed for improving the flatness of hot strip. Flatness profile induces the flatness of hot strip in the lateral direction using the second coefficient of quadratic equation. The FlatSIL system was established in real plant. An operator who works in the field can monitor the flatness of hot strip during hot rolling processes. The designed GMV S-T PI controller was implemented in hot finishing mill processes. As shown in experimental results, the improved flatness performances were shown. However, it is found that it is hard to control the flatness of thinner strip, because continuously control input is saturated. In order to enhance the better flatness performance, the bender actuator's capacity should be increased.

### References

Astrom, K. J. and Wittenmark, B., 1973, "On Self-Tuning Regulator," *Automatica*, Vol. 9, pp. 185~199.

Gawthrop, P., 1986, "Self-Tuning PID Controllers: Algorithms and Implementation," *IEEE Transactions on Automatic Control*, Vol. 31,



Issue. 3, pp. 201~209.

Xilin, Y., Hui, M., Zhongyi, Q. and Guofan, J., 1997, "Image Processing System in Shape Meter for Hot Strip Mill," IEEE International Conference on Intelligent Processing Systems, pp. 1027~1030.

Yamamoto, T., 1999, "Generalized Minimum Variance Self-Tuning Pole-Assignment Controller with a PID Structure," Proceeding of the IEEE International Conference on Control Ap-

plication, pp. 125~130.

Yang, X. and Jiao, J., 1973, "Development and Research of Multi-beam Laser Shape Meter for Hot Rolled Strip," Metallurgical Industry Automation, pp. 24~28.

Yi, J. J. and Hong, W. K., 2001, "Challenges for the Asian Steel Industry in the New Era," South East Asia Iron & Steel Institute, Singapore, pp. 1~10.